LUND UNIVERSITY

Microchip electroseparation of proteins using lipid-based nanoparticles

Ohlsson, Pelle; Ordeig, Olga; Nilsson, Christian; Harwigsson, Ian; Kutter, Jorg P.; Nilsson, Staffan

Microchip electroseparation of proteins using lipid-based nanoparticles

SCHOLARONE™
Manuscripts

1
2
3
4
5
6
7
8
9
10
11
12
13
14
15
16
17
18
19
20
21
22
23
24
25
26
27
28
29
30
31
32
33
34
35
36
37
38
39
40
41
42
43
44
45
46
47
48
49
50
51
52
53
54
55
56
57
58
59
60

Title: Microchip electroseparation of proteins using lipid-based nanoparticles

Authors: Pelle Ohlsson*[,1], Olga Ordeig*[,1], Christian Nilsson[2], Ian Harwigsson[3], Jörg P.

Kutter[1], Staffan Nilsson[2]

*Contributed equally

[1]Department of Micro and Nanotechnology, Technical University of Denmark, Kongens

Lyngby, Denmark

[2]Pure and Applied Biochemistry, Center of Chemistry and Chemical Engineering, Lund

University, Lund, Sweden

[3]Camurus AB, Lund, Sweden

Corresponding author: Christian Nilsson, Pure and Applied Biochemistry, Center of

Chemistry and Chemical Engineering, Lund University, P.O. Box 124, SE-221 00 Lund,

Sweden. E-mail: christian.nilsson@tbiokem.lth.se. Fax: +46 46 222 4611.

Abbreviations: COC, cyclic olefin copolymer, **COP**, cyclic olefin polymer, **cryoTEM**,

cryogenic transmission electron microscopy, **GFP**, green fluorescent protein, **HEC**,

hydroxyethyl cellulose, **PEGMA**, poly(ethylene glycol) methacrylate, **PSP**, pseudostationary

phase

Keywords: Adsorption reduction / Lipid-based nanoparticles / Microchip electrophoresis /

Microfluidics / Protein separation

Total number of words: 4503

ABSTRACT

Porous liquid crystalline lipid-based nanoparticles are here shown to enable protein analysis in microchip electroseparation by reducing sample adsorption. Additionally, higher stability and reproducibility of the separations were observed. The method was tested by separating green fluorescent protein (GFP) in hot embossed cyclic olefin polymer microchips with integrated fiber grooves for laser-induced fluorescence detection. The sample adsorption was indirectly quantified by measuring the height, width and asymmetry of the separation peaks for various concentrations of nanoparticles in the sample and background electrolyte. Without nanoparticles, electropherograms displayed typical signs of extensive adsorption to the channel walls, with low, broad, tailing peaks. Higher, narrower more symmetric peaks were generated when 0.5-10 % nanoparticles were added, showing a dramatic reduction of sample adsorption. The current through the separation channel decreased with nanoparticle concentration, reducing to half its value when the nanoparticle concentration was increased from 0.5 to 4 %. Addition of nanoparticles enabled separations that were otherwise hindered by extensive adsorption, e.g. separation of GFP mutants differing by only one amino acid. It was also observed that increasing the nanoparticle concentration increased the number of impurities that could be resolved in a GFP sample. This indicates that the adsorption is further reduced, and/or that the nanoparticles provide an interacting pseudostationary phase (PSP) for electrochromatography.

1 INTRODUCTION

Electro-driven separation methods can be used to separate a wide range of substances, from small molecules to DNA and proteins [1]. Protein separations are, however, often hampered by extensive sample adsorption to the channel walls. Two approaches are mainly used to solve this problem: either dynamic coatings that are added to the liquids flowing through the channels, or surface modifications of the channel walls (e.g. covalent attachment of molecules, UV or oxygen plasma treatment) [2, 3].

The choice of method to reduce adsorption is highly dependent on the substrate material. Several methods have been developed for common chip materials, such as glass, PMMA and PDMS [2, 3]. Lately, cyclic olefin polymers (COPs) and cyclic olefin copolymers (COCs) have become popular substrate materials for microfluidics due to their high chemical resistance, good optical quality and suitability for mass production [4]. Methods to reduce protein adsorption to these materials are not yet as thoroughly investigated, although photografting of poly(ethylene glycol) methacrylate (PEGMA) [5] and dynamic coating of hydroxyethyl cellulose (HEC) [6] have been successfully employed in COC chips. Recently, it was observed that addition of porous lipid-based liquid crystalline nanoparticles to the background electrolyte enabled separation of green fluorescent protein (GFP) in COC capillaries by providing an interaction phase either at the microchip surface or in bulk solution [7]. These results inspired us to investigate the possibility of transferring this method to microfluidic chips made from COP, which is chemically similar to COC. There are several important differences between the capillary and chip systems, which could affect the suppression of the adsorption. First of all, the surface properties are different, since the material has a different chemical composition and another fabrication method was used. Secondly, the channels have a rectangular cross-section instead of a circular one. Thirdly, the

gated electrokinetic injections used in the microchip might affect the charged sample molecules and nanoparticles.

Various kinds of nanoparticles have been used extensively for separations both in capillaries and chips, primarily as pseudostationary phase (PSP) for electrochromatography or as surface coating [8-10]. Using nanoparticles as pseudostationary phase [9-11] is an elegant alternative to other electrochromatography formats, e.g. coated open channels [12, 13], packed beds [14], *in situ* polymerized porous monolithic columns [15] and microfabricated support structures [16-19]. When nanoparticles are used as PSP, they are suspended in the electrolyte solution and continuously pumped through the capillary by the electroosmotic flow during separation. Thereby the nanoparticles are used only once and adsorption of sample or sample matrix to the nanoparticles does not affect subsequent separations, minimizing the need for column regeneration.

The particles used in this work are lipid-based liquid crystalline nanoparticles [7, 20-22]. They are prepared by a one-step procedure based on lipid self assembly, and benefit from small size, high porosity, as well as large variety of surface chemistries available. Advantages of lipid-based nanoparticles also include their compatibility with proteins and suspension stability at high concentration. Their topography, size and surface characteristics have been further investigated as reported in references [7] and [22]. Briefly, the nanoparticles have an average hydrodynamic diameter of 70 nm and are composed of a "melted" bicontinuous cubic phase. These nanoparticles have previously been used as PSP for CEC in fused-silica capillaries [22, 23] and to reduce protein adsorption in COC capillaries [7]. The present work is, to the best of our knowledge, the first time nanoparticles have been used as a suspended interaction phase in microchip electroseparations of proteins.

In this work, porous liquid crystalline lipid-based nanoparticles were used to enable microchip electroseparation of GFP. The results indicate that the nanoparticles enable separation by reducing sample adsorption to the channel wall, and may provide a pseudostationary phase for chromatography. Additionally, they were found to reduce current through the separation channel. The measurements were performed in hot embossed cyclic olefin polymer chips with integrated fibercouplers for LIF detection.

2 MATERIALS AND METHODS

2.1 Chemicals

Tricine buffer (50 mM, pH 7.5), mixed with different concentrations of lipid-based nanoparticles, ranging from 0 to 10%, was used for all experiments. Sodium hydroxide solution (Fluka, Schnelldorf, Germany) at 0.1 M and ethanol (70 %, Sigma-Aldrich, Steinheim, Germany) were used for conditioning of the microchannels. Tricine was obtained from Sigma-Adrich (St. Louis, MO, USA) and isopropanol was purchased from Sigma-Adrich (Steinheim, Germany). All solutions were mixed with ultra pure water from a Milli-Q filtration systems (Millipore, Billerica, MA, USA).

2.2 Preparation and characterization of lipid-based nanoparticles

The preparation of the lipid-based liquid crystalline nanoparticles has been described elsewhere [22]. In brief, a preformulation composed of lipids (soy phosphatidylcholine, glycerol dioleate and polysorbate 80), oleic acid and ethanol was added to water. The mixture was then stirred for 48 hours at room temperature to form an aqueous nanoparticle suspension (20 % w/w), which was filtered through a sterile filter and stored at room temperature until

further used. The nanoparticle stock solution contained 2 % ethanol, causing a trace of 0-1 %

ethanol in the sample and background electrolyte solutions. The number-averaged

hydrodynamic diameter for the nanoparticles was 70 nm, according to dynamic light

scattering measurements [7, 22]. This agreed well with cryogenic transmission electron

microscopy (cryoTEM) images, showing a geometric diameter of 50-100 nm (see Figure 1).

The topography, size and surface characteristics of the nanoparticles are further described and

discussed in references [7] and [22].

2.3 Preparation of GFP samples

All samples contained either native GFP or a mixture of two GFP mutants with one amino

acid substituted. The two mutants had a neutral asparagine residue (N212) replaced by either a

positive lysine residue (N212K) or a negative glutamate residue (N212E). They are

henceforth referred to as (+)GFP and (-)GFP, respectively. The GFP was dissolved in 50 mM

tricine buffer with the same concentrations of lipid-based nanoparticles as in the background

electrolyte used in each experiment. The construction, expression, selection and pretreatment

of the GFP mutants is described in reference [22]. In short, the *gfpuv* gene was amplified by

PCR using plasmid pTGFPuv as template. Complementary oligonucleotides carrying

mismatches were used for the construction of GFP N212K and GFP N212E. After digestion

of the template DNA with *Dpn*I for 1 h at 37 °C, the newly constructed plasmids were

transformed into *E. coli* competent cells and grown overnight on modified Luria-Bertani agar

plates. The colonies showing fluorescence under UV light were selected and the sequence was

confirmed by DNA sequencing before transferring the colonies to shake flasks. The cells were

grown overnight at 30°C with vigorous shaking, harvested by centrifugation, resuspended and

lysed by sonication. The extracts of GFP were purified by heat treatment (70°C, 10 minutes),

subjected to salt precipitation (1.5 M to 2.8 M ammonium sulphate), resuspended and

dialyzed overnight. The final stock solution contained 50 mM phosphate buffer (pH 7.0),

which added a trace of phosphate buffer to the samples used in the experiments.

2.4 Microfluidic chip design

A schematic of the layout and a photograph of the chip are shown in Figures 2a and 2b,

respectively. The fluidic network consisted of an injection cross and a 34-mm-long separation

channel followed by a 1-mm-long Z-shaped detection cell. The detection cell is coupled to an

optical fiber through a fiber coupling groove fabricated in the same procedure as the channels;

the diameter of the fiber thus sets a lower limit for the depth of the channels. All channels are

approximately 80 μm wide and 80 μm deep. The lengths of the sample, sample waste and

buffer channels were 10 mm, which was estimated as the minimal length needed to limit the

pressure driven flow due to changing liquid levels in the reservoirs.

2.5 Chip fabrication

The microchip was fabricated through the assembly of two COP parts, a lower part containing

the microfluidic channels and the optical fiber coupling grooves and an upper part containing

the access holes to the microfluidic system. Both parts were fabricated from 188-µm-thick

COP sheets (Zeonor 1420R), which were kindly provided by Zeon Corporation, Japan.

The bottom part of the device, which contained the microfluidic channels and the fiber

coupling grooves, was structured in the COP sheet by hot embossing. For that, a silicon

master was fabricated using standard UV-lithography and Bosch-type deep reactive ion-

etching. More details regarding the master fabrication process can be found in reference [16].

The last step of the master fabrication was the deposition of a 1H,1H,2H,2H-

perfluorodecyltrichlorosilane layer by chemical vapor deposition (MVD 100, Applied

Microstructures Inc., USA) as an antisticking coating. This facilitated the release of the

microstructured COP sheet from the master. The chips were individually cut from the wafer

with a dicing saw and cleaned with isopropanol before being used as master for hot

embossing.

The master and a clean COP sheet, previously cut to the chip dimensions (8 x 3 cm), were

placed in a manual laboratory bonding press with high temperature cooling plates

(TEMPRESS, Paul-Otto Weber GmbH, Germany). COP was embossed at 170 °C and 10 kN

for 10 minutes. De-embossing of the system was performed at 50 °C to avoid deformations of

the microstructures.

In parallel to the microchannel hot embossing, another COP sheet was cut to the chip

dimensions and 2 mm diameter holes were manually drilled to access the microfluidic

network. The final closed channel configuration was achieved by bonding the two COP parts.

Prior to this step, the surfaces of both parts were carefully cleaned with isopropanol for 15

minutes in an ultrasonic bath. After rinsing in deionized water and drying with a nitrogen gun,

both parts were placed in contact and bonded at 120 °C and 10 kN for 10 minutes in the same

hot press used for embossing. The bonding temperature was chosen slightly under the glass

transition temperature of the COP (136 °C) to avoid collapse of the channels. Finally, glass

reservoirs were glued on top of the lid using UV-curable glue (Norland Optical Adhesive 68,

Norland Products, Cranbury, NJ, USA).

2.6 Setup and instrumentation

Figure 2c shows a schematic illustration of the experimental setup. A blue (488 nm) argon ion

laser (543-AP, Melles Griot, Carlsbad, CA, USA) was used as light source and coupled to the

chip by an optical fiber. The optical fiber used in this work had a 51 μm pure silica core and

an outer diameter of 67 μm (FVP050055065, Polymicro Technologies, Phoenix, AZ, USA).

The fiber was inserted into an integrated fiber coupler in the chip launching the light along the

length of the detection cell. Fluorescence from the detection cell was collected vertically

through the cover lid by a microscope objective (M-20X, Newport, Irvine, CA, USA) and

detected by a photomultiplier tube (PMT, R1617, Hamamatsu, Japan). The background from

scattered excitation light was suppressed by detection perpendicular to the excitation source

and filtering through two long-pass filters with a cut-off wavelength of 500 nm (FEL0500,

Thorlabs, Sweden). The signal was amplified and low-pass filtered (10 Hz cut-off, -12

dB/octave) by a current preamplifier (SR570, Stanford Research Systems, Sunnyvale, CA,

USA). It was then digitized and collected on a computer at 100 Hz (LabJack U12 and

LJstream, LabJack Corporation, Lakewood, CO, USA). The fluidic flow in the chip was

controlled electrokinetically by electrodes in the reservoirs connected to an in-house built

power supply. The power supply was in turn controlled by in-house written Lab VIEW 6.1

(National Instruments, Austin, TX, USA) software. The current through the separation

channel was measured by a picoammeter (485, Keithley Instruments Inc., Cleveland, OH,

USA) connected to the buffer waste reservoir.

2.7 Experimental methods

The chip was conditioned before each measurement series with a sequence of water, 70 %

ethanol, water, 100 mM sodium hydroxide solution and water, pumped by suction for at least

2 minutes each. Finally, the chip was filled by suction with background electrolyte containing

the same concentration of nanoparticles as the sample. Sample was injected into the

separation channel by 1-s-long gated injections [24] and separated at field strengths of 255 V/cm.

2.8 Data treatment

The retention time, peak height, peak width and peak asymmetry were measured in an in-house written Matlab script (The MathWorks Inc., Natick, MA, USA). The data were first smoothened with a moving average smoother with a width of 0.5 s, except for data for 0 % nanoparticles, which was smoothened with a width of 5 s to compensate for lower signal-to-noise ratio. Peak height was measured from baseline to maximum value. Peak width and asymmetry were measured at half-peak height, since impurities that were not completely separated prevented measurement at lower height. Peak asymmetry was calculated as the time from the maximum of the peak to the half-height of the tail, divided by the time from the half height of the front to the maximum of the peak.

3 RESULTS AND DISCUSSION

3.1 Reduction of adsorption

As lipid-based nanoparticles have previously been observed to enable protein analysis in COC capillaries by reducing sample adsorption to the walls [7], we here analyze this effect for electroseparation in COP microchips, which have similar material properties. GFP was chosen as protein analyte due to its native fluorescence, which enables detection without labeling. It is a protein of high interest, since it is extensively used in molecular and cellular biology. The sample adsorption was measured indirectly by measuring typical signs of adsorption, such as peak broadening, peak asymmetry and decrease of peak height when various concentrations of nanoparticles were added to both the sample and background electrolyte.

A GFP sample at a concentration of 0.3 mg/ml was separated in 50 mM tricine buffer (pH 7.5), with 0-10 % nanoparticles. The sample solution was electrokinetically injected by 1 s gated injections and separated in field strengths of 255 V/cm. Examples of separations at different nanoparticle concentrations are shown in Figure 3.

Separations without nanoparticles showed typical signs of substantial sample adsorption, with low, broadened, tailing peaks. Measurements using 0-0.25 % nanoparticles were very unstable, with large variations in current through the separation channel, fluorescence background and peak height and shape. Therefore, results obtained without nanoparticles are very uncertain. The results for 0.25 % nanoparticles were not reproducible and were thus omitted.

Adding 0.5-10 % nanoparticles to the sample and background electrolyte decreased adsorption and increased the reproducibility of the separations. The retention time was more reproducible compared to measurements without nanoparticles. The peak height was increased approximately ten times when adding 0.5-2 % nanoparticles (Figure 4a). For higher concentrations it decreased again, probably due to scattering of excitation light by the nanoparticles in the detection cell. The peak shape was also affected, with roughly 10 times narrower peaks when using 0.5-10 % nanoparticles (Figure 4b). Peak asymmetry continuously decreased with nanoparticle concentrations up to 2 % (Figure 4c).

The addition of nanoparticles reduced GFP adsorption to the channel walls. It has not yet been investigated thoroughly how general this effect is for various proteins, but it is not likely to be unique for GFP. It has been suggested that the nanoparticles shield interaction sites at the channel walls, or that interaction with the large surface area of the nanoparticles outcompetes

adsorption [7]. The interaction could be either electrostatic, hydrophobic or sieving through

the pores of the nanoparticles. Hydration of the nanoparticles and adsorption of ions from the

electrolyte may affect the interaction. However, it is not yet possible to draw any definite

conclusions about the mechanism from the present measurements.

3.2 Reduction of current

It was observed that the current through the separation channel decreased with increasing

nanoparticle concentration, as shown in Figure 4d. The decrease was significant, with the

current roughly halved when increasing the nanoparticle concentration from 0.5 to 4 %. In

this range, retention time was not affected. Again, the measurements with 0-0.25 %

nanoparticles were unstable and did not yield any reproducible result.

The origin of the reduction of current is not known, but it can be speculated that the

nanoparticles accumulate around the anode and thus reduce its effect, change the dielectric

constant of the bulk electrolyte, or affect the ionic strength by adsorbing ions from the

electrolyte. Since Joule heating caused by the current flowing through the separation channel

is a limiting factor for electrodriven separations, the effect of drastically decreasing the

current without increasing the time for the separation is potentially very useful.

3.3 Effect on optical detection

We expected the scattering of excitation light by the lipid-based nanoparticles in the detection

cell to increase the fluorescence baseline. Surprisingly, the baseline was essentially

independent of nanoparticle concentration, as can be seen in Figure 3a. This shows that the

two longpass filters used to filter out the fluorescence light effectively suppressed any

scattered excitation light. The baseline is consequently a result of other effects, e.g.,

autofluorescence of the chip material.

An increase in the nanoparticle concentration and thereby the scattering of excitation light out

of the detection cell reduced the fluorescence signal. Combined with the opposite effect of

increased peak height from reduced sample adsorption, this gives a maximum peak height

when 0.5-2 % nanoparticles are used (see Figure 4a).

Even though the baseline level is independent of nanoparticle concentration, the noise

(measured as the standard deviation) of the baseline increases with nanoparticle concentration,

especially from 0 to 1 % nanoparticles. In combination with the previously mentioned effects,

this gives an optimal signal-to-noise ratio of approximately 900 for 0.3 mg/ml GFP at 0.5 %

nanoparticles. The theoretical limit of detection (S/N=3) for GFP is thus 1 µg/ml. This shows

that LIF can provide low limits of detection also when nanoparticles are present. To

completely circumvent the adverse effects on optical detection, it would certainly be possible

to employ other methods of detection, e.g. electrochemical detection or mass spectrometry

(MS) [25].

3.4 Effect on separations

To demonstrate the practical use of lipid-based nanoparticles in protein separations, two

example separations were performed. First, GFP was separated from impurities in 50 mM

tricine buffer (pH 7.5) containing 0-10 % nanoparticles. When no nanoparticles were added,

GFP could not be analyzed, due to extensive peak broadening caused by adsorption (see

Figure 3). Adding 0.5-10 % nanoparticles made it possible to resolve the main GFP peak from

peaks caused by impurities. Increasing nanoparticle concentration increased the number of

detectable impurities. This could be due to further reduction of adsorption, or an increasing

chromatographic effect, where the nanoparticles would work as pseudostationary phase. The

plate height for the main peak was 1 mm with no nanoparticles present, but in the range of

only 8-18 µm for 0.5-10 % nanoparticles.

As a second separation example two GFP variants, (+)GFP and (-)GFP, were separated. They

differ by only one amino acid that has been substituted with a positive and negative amino

acid, respectively. Again, the peaks could only be resolved when nanoparticles were added to

the background electrolyte (Figure 5). It was observed that the resolution of the two peaks

increased while the peak height decreased with increasing buffer concentration in the range of

10-50 mM. Increasing the buffer concentration reduces the electroosmotic flow, which

increases the time spent by the analytes in the electric field, which in turn increases their

electrophoretic separation. Increasing the buffer concentration also promotes the interaction

between the proteins, nanoparticles and capillary walls, by shielding their negative charge and

thus reducing the electrostatic repulsion [22]. This could increase sample adsorption to the

walls, explaining the lower peaks. It would also increase any chromatographic effect of the

nanoparticles, which is another possible explanation of the increased resolution.

4 CONCLUDING REMARKS

Porous liquid crystalline lipid-based nanoparticles enable electroseparation of proteins in COP

microchips and add positive effects such as higher stability and reproducibility, and decreased

current. From the present measurements it is clear that the lipid-based nanoparticles reduce

GFP adsorption to the COP channel walls of the microchip. This agrees well with previous

measurements in COC capillaries, where the GFP sample was only recovered in the presence

of the nanoparticles [7], and shows that the method can also be used in the microchip format,

with COP as substrate material and with gated electrokinetic injections. The investigations

show that lipid-based nanoparticles are a potent buffer additive to reduce sample adsorption in

both capillary and microchip separations. Further research is required to fully understand the

generality and mechanism of the effect.

The role of lipid-based nanoparticles as pseudostationary phase for electrochromatography

has previously been investigated in fused-silica capillaries [22]. In the present measurements,

however, the relative importance of the electrophoretic and chromatographic effects is not yet

clear. It would be interesting to further investigate lipid-based nanoparticles as

pseudostationary phase for microchip electrochromatography. Reducing the channel

dimensions of the chip would improve heat dissipation and make it possible to use higher

buffer concentrations, which would promote chromatographic interactions. The effect would

also be easier to investigate in glass chips, where sample adsorption usually interferes less

with the measurements.

5 REFERENCES

[1] Wu, D. P., Qin, J. H., Lin, B. C., *J. Chromatogr. A* 2008, *1184*, 542-559.

[2] Dolnik, V., *Electrophoresis* 2004, *25*, 3589-3601.

[3] Muck, A., Svatos, A., *Talanta* 2007, *74*, 333-341.

[4] Nunes, P. S., Ohlsson, P. D., Ordeig, O., Kutter, J. P., *Microfluid. Nanofluidics* 2010, *9*, 145-161.

[5] Stachowiak, T. B., Mair, D. A., Holden, T. G., Lee, L. J., Svec, F., Frechet, J. M. J., *J. Sep. Sci.* 2007, *30*, 1088-1093.

[6] Zhang, J., Das, C., Fan, Z. H., *Microfluid. Nanofluidics* 2008, *5*, 327-335.

[7] Nilsson, C., Harwigsson, I., Becker, K., Kutter, J. P., Birnbaum, S., Nilsson, S., *Electrophoresis* 2010, *31*, 459-464.

[8] Guihen, E., Glennon, J. D., *Anal. Lett.* 2003, *36*, 3309-3336.

[9] Nilsson, C., Birnbaum, S., Nilsson, S., *J. Chromatogr. A* 2007, *1168*, 212-224.

[10] Nilsson, C., Nilsson, S., *Electrophoresis* 2006, *27*, 76-83.

[11] Wallingford, R. A., Ewing, A. G., *Adv. Chromatogr.* 1989, *29*, 1-76.

[12] Kutter, J. P., Jacobson, S. C., Matsubara, N., Ramsey, J. M., *Anal. Chem.* 1998, *70*, 3291-3297.

[13] Jacobson, S. C., Hergenroder, R., Koutny, L. B., Ramsey, J. M., *Anal. Chem.* 1994, *66*, 2369-2373.

[14] Oleschuk, R. D., Shultz-Lockyear, L. L., Ning, Y. B., Harrison, D. J., *Anal. Chem.* 2000, *72*, 585-590.

[15] Ericson, C., Holm, J., Ericson, T., Hjerten, S., *Anal. Chem.* 2000, *72*, 81-87.

[16] Gustafsson, O., Mogensen, K. B., Kutter, J. P., *Electrophoresis* 2008, *29*, 3145-3152.

[17] Gustafsson, O., Mogensen, K. B., Ohlsson, P. D., Liu, Y., Jacobson, S. C., Kutter, J. P., *J. Micromech. Microeng.* 2008, *18*.

[18] He, B., Tait, N., Regnier, F., *Anal. Chem.* 1998, *70*, 3790-3797.

[19] Pumera, M., *Talanta* 2005, *66*, 1048-1062.

[20] Johnsson, M., Barauskas, J., Norlin, A., Tiberg, F., *J. Nanosci. Nanotechnol.* 2006, *6*, 3017-3024.

[21] Landau, E. M., Rosenbusch, J. P., *Proc. Natl. Acad. Sci. U.S.A.* 1996, *93*, 14532-14535.

[22] Nilsson, C., Becker, K., Harwigsson, I., Bulow, L., Birnbaum, S., Nilsson, S., *Anal. Chem.* 2009, *81*, 315-321.

[23] Nilsson, C., Harwigsson, I., Birnbaum, S., Nilsson, S., *Electrophoresis* 2010, *31*, 1773-1779.

[24] Jacobson, S. C., Koutny, L. B., Hergenroder, R., Moore, A. W., Ramsey, J. M., *Anal. Chem.* 1994, *66*, 3472-3476.

[25] Nilsson, C., Viberg, P., Spegel, P., Jornten-Karlsson, M., Petersson, P., Nilsson, S., *Anal. Chem.* 2006, *78*, 6088-6095.

ACKNOWLEDGEMENTS

CONFLICT OF INTEREST STATEMENT

The authors declare no conflict of interest.

FIGURE CAPTIONS

Figure 1. Cryogenic transmission electron microscopy (cryoTEM) image of the lipid-based

nanoparticles used to reduce protein adsorption. The imaging procedure can be found in

reference [22].

Figure 2. (A) Layout of the CE microchip used in this work. The separation channel is 34 mm

long, 80 µm wide and 80 µm deep. The Z-shaped detection cell is 1 mm long. (B) Picture of

the chip. (C) Schematic of the setup.

Figure 3. Electropherograms showing the GFP peak shape for various nanoparticle

concentrations. GFP at a concentration of 0.3 mg/ml was separated in 50 mM tricine buffer

(pH 7.5), with 0, 2 and 10 % nanoparticles added to both the sample and background

electrolyte. Separation voltage was 255 V/cm and injection time was 1 s. Electropherograms

are offset vertically for clarity.

Figure 4. Plots showing how the separation characteristics vary with nanoparticle

concentration. (A) Peak height (black) and baseline level (gray). (B) Full-width at half-

maximum (FWHM) of peaks. (C) Peak asymmetry. (D) Current through separation channel.

All plots show average and ± standard deviation of three repeated measurements. Details of

the measurements and data treatment are given in the text.

Figure 5. Separation of two GFP mutants, (+)GFP and (-)GFP, enabled by addition of lipid-

based nanoparticles. The mutants differ by only one amino acid that has been substituted with

a positive and negative amino acid respectively. Separation performed in 50 mM tricine

buffer (pH 7.5) with 1 % nanoparticles added to both the sample and background electrolyte.

Separation voltage was 255 V/cm and injection time was 1 s.

1
2
3
4
5
6
7
8
9
10
11
12
13
14
15
16
17
18
19
20
21
22
23
24
25
26
27
28
29
30
31
32
33
34
35
36
37
38
39
40
41
42
43
44
45
46
47
48
49
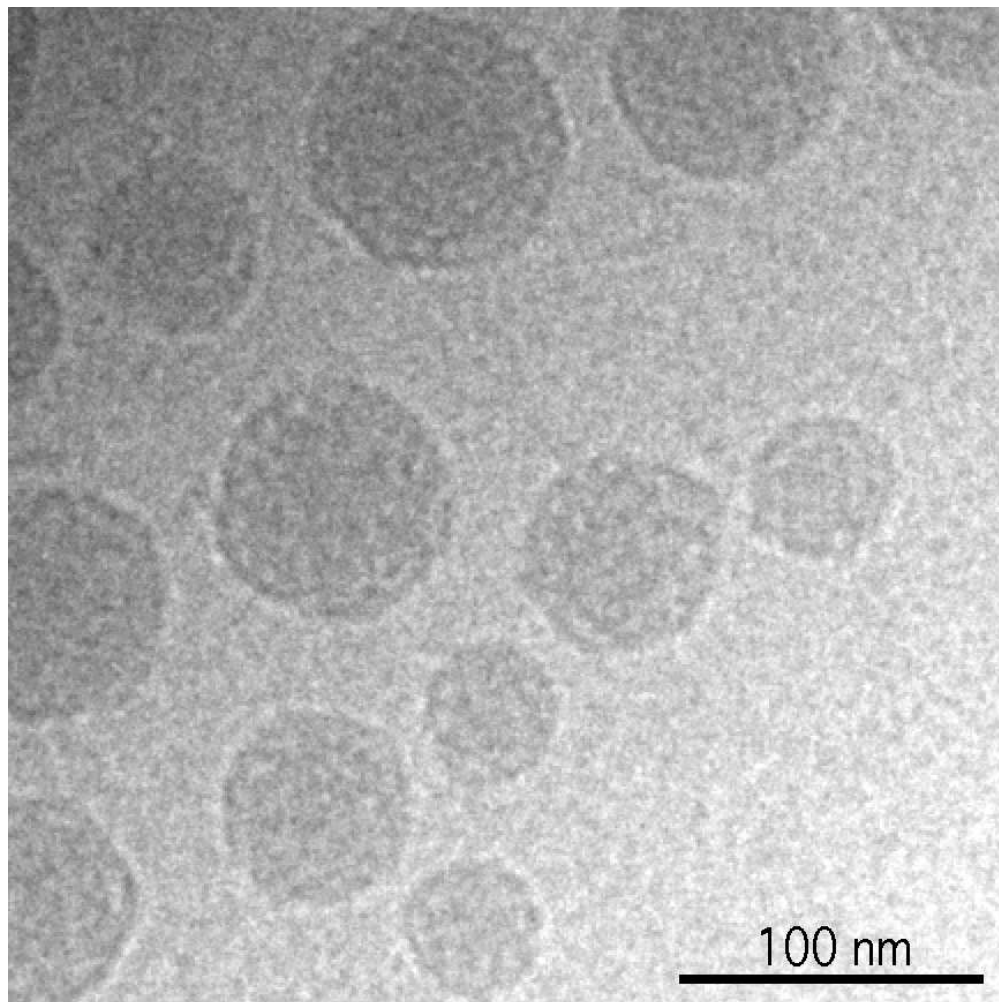50
51
52
53
54
55
56
57
58
59
60

Figure 1. Cryogenic transmission electron microscopy (cryoTEM) image of the lipid-based nanoparticles used to reduce protein adsorption. The imaging procedure can be found in reference [22].
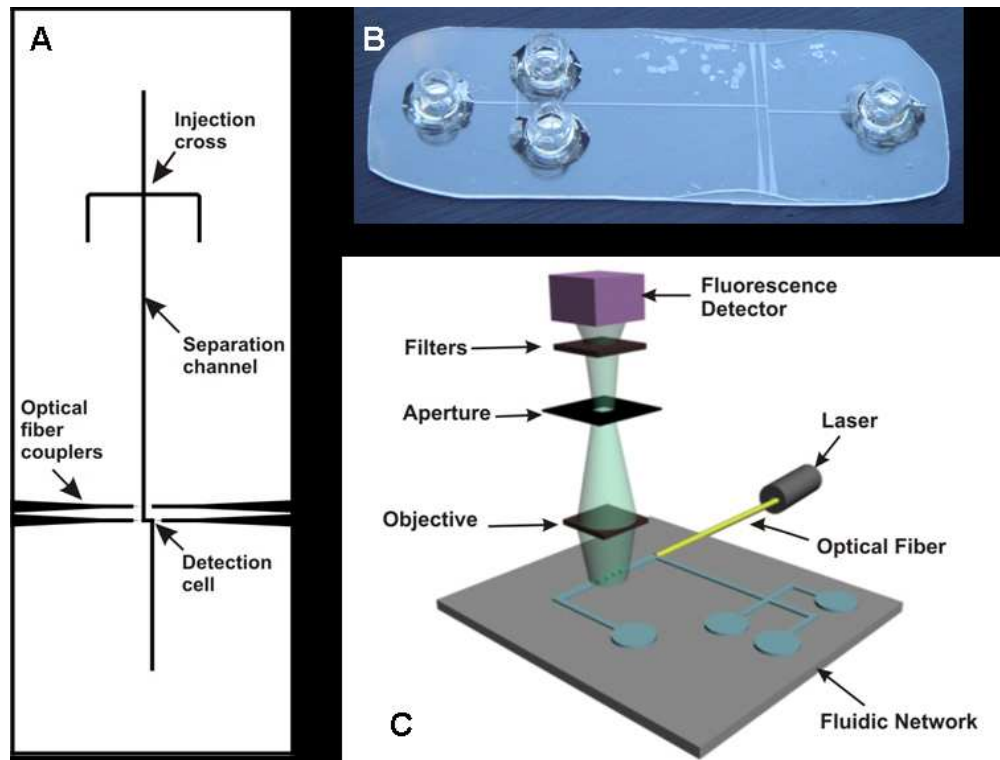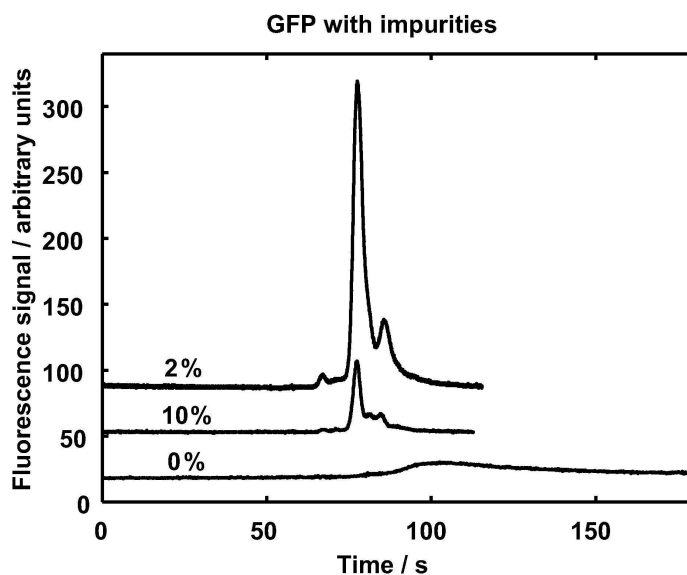79x79mm (276 x 276 DPI)

Figure 2. (A) Layout of the CE microchip used in this work. The separation channel is 34 mm long, 80 µm wide and 80 µm deep. The Z-shaped detection cell is 1 mm long. (B) Picture of the chip. (C) Schematic of the setup.
128x97mm (150 x 150 DPI)

Figure 3. Electropherograms showing the GFP peak shape for various nanoparticle concentrations. GFP at a concentration of 0.3 mg/ml was separated in 50 mM tricine buffer (pH 7.5), with 0, 2 and 10 % nanoparticles added to both the sample and background electrolyte. Separation voltage was 255 V/cm and injection time was 1 s. Electropherograms are offset vertically for clarity.
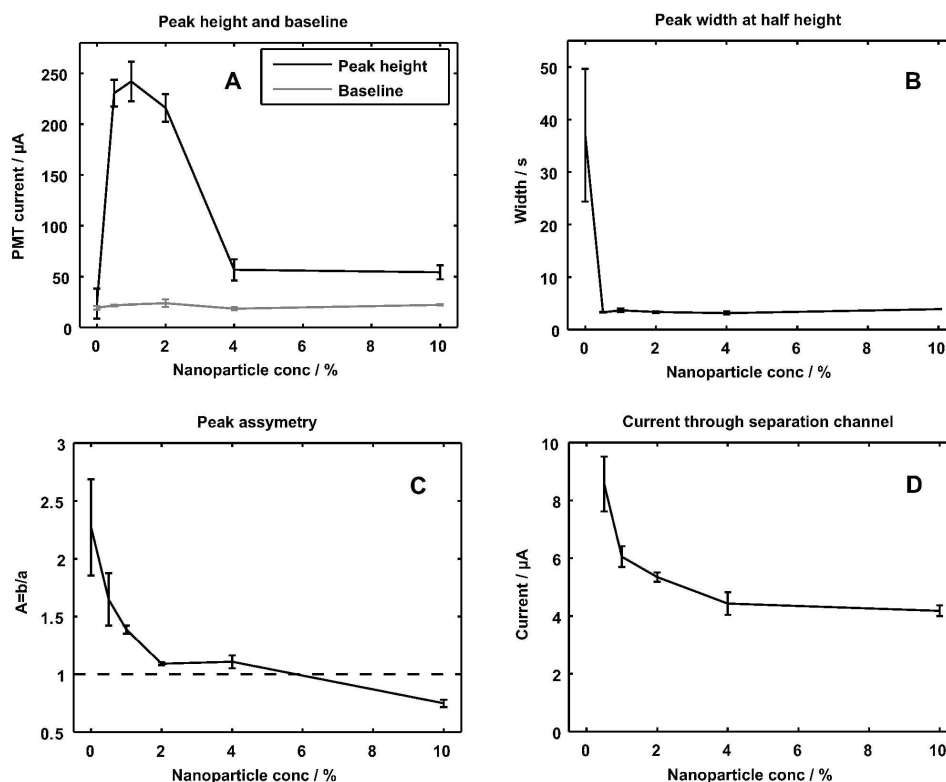114x92mm (600 x 600 DPI)

Figure 4. Plots showing how the separation characteristics vary with nanoparticle concentration. (A) Peak height (black) and baseline level (gray). (B) Full-width at half-maximum (FWHM) of peaks. (C) Peak asymmetry. (D) Current through separation channel. All plots show average and ± standard deviation of three repeated measurements. Details of the measurements and data treatment are given in the text.
177x186mm (600 x 600 DPI)
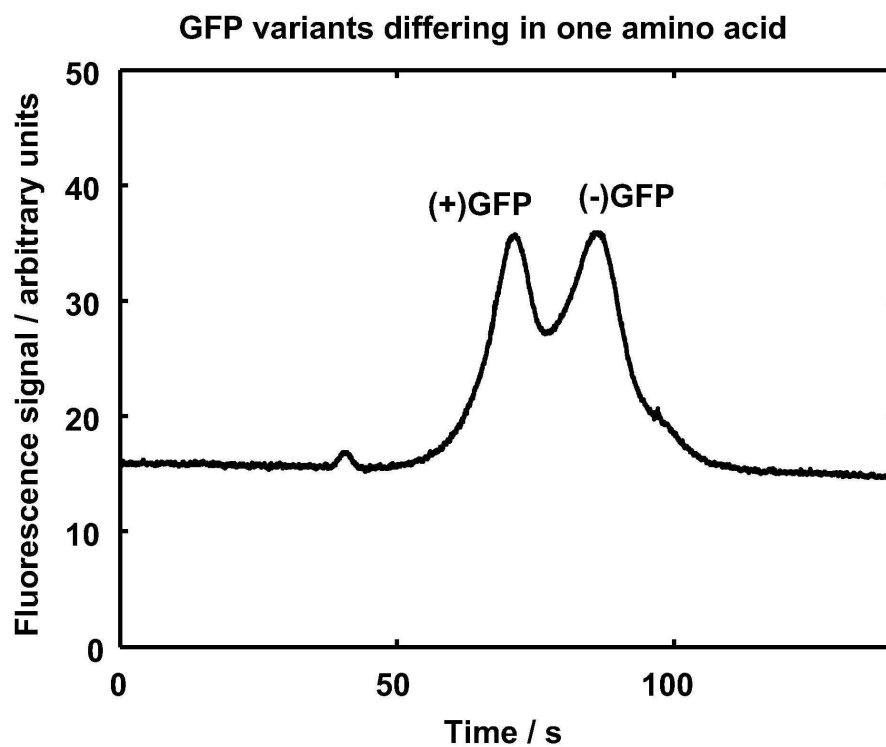
1
2
3
4
5
6
7
8
9
10
11
12
13
14
15
16
17
18
19
20
21
22
23
24
25
26
27
28
29
30
31
32
33
34
35
36
37
38
39
40
41
42
43
44
45
46
47
48
49
50
51
52
53
54
55
56
57
58
59
60

Figure 5. Separation of two GFP mutants, (+)GFP and (-)GFP, enabled by addition of lipid-based nanoparticles. The mutants differ by only one amino acid that has been substituted with a positive and negative amino acid respectively. Separation performed in 50 mM tricine buffer (pH 7.5) with 1 % nanoparticles added to both the sample and background electrolyte. Separation voltage was 255 V/cm and injection time was 1 s.
88x66mm (600 x 600 DPI)